AIP | Journal of Applied Physics

Unification of three multiphonon trap-assisted tunneling mechanisms

Manhong Zhang, Zongliang Huo, Zhaoan Yu, Jing Liu, and Ming Liu

Citation: J. Appl. Phys. **110**, 114108 (2011); doi: 10.1063/1.3662195
View online: http://dx.doi.org/10.1063/1.3662195
View Table of Contents: http://jap.aip.org/resource/1/JAPIAU/v110/i11
Published by the AIP Publishing LLC.

Additional information on J. Appl. Phys.

Journal Homepage: http://jap.aip.org/
Journal Information: http://jap.aip.org/about/about_the_journal
Top downloads: http://jap.aip.org/features/most_downloaded
Information for Authors: http://jap.aip.org/authors

ADVERTISEMENT

Downloaded 05 Sep 2013 to 35.8.11.2. This article is copyrighted as indicated in the abstract. Reuse of AIP content is subject to the terms at: http://jap.aip.org/about/rights_and_permissions

Unification of three multiphonon trap-assisted tunneling mechanisms

Manhong Zhang,[a] Zongliang Huo, Zhaoan Yu, Jing Liu, and Ming Liu
Laboratory of Nanofabrication and Novel Device Integration, Institute of Microelectronics, Chinese Academy of Sciences, Beijing 100029, People's Republic of China

(Received 12 May 2011; accepted 16 October 2011; published online 2 December 2011)

There are three basic multiphonon trap-assisted tunneling (TAT) mechanisms in the gate leakage current of a metal-oxide-semiconductor (MOS) structure: the short-ranged trap potential, nonadiabatic interaction and electric field induced trap-band transitions. In this paper, a comparison of these three mechanisms is made for the first time in a single (Schenk's model) MOS structure. A properly box-normalized electron wave function in the SiO_2 conduction band in an electric field is used to calculate the field ionization rate of a deep neutral trap. It is found that capture and emission rates of a deep neutral trap are almost the same in the short-ranged trap potential and nonadiabatic interaction induced TAT processes, so the two mechanisms give a similar contribution to the total TAT current. The calculated TAT current and the average relaxation energy (~1.5 eV) due to these two mechanisms are in good agreement with the experimental results. In contrast, capture and emission rates in Schenk's model are several orders smaller. The TAT current induced by this mechanism is also much smaller and can be ignored. © *2011 American Institute of Physics*. [doi:10.1063/1.3662195]

I. INTRODUCTION

Stress-induced leakage current (SILC) in thin SiO_2 and high-k dielectrics is one of the most crucial reliability concerns in complementary metal-oxide-semiconductor (CMOS) devices.[1] A lot of experimental and theoretical work have been done to explain its mechanisms. The reason of SILC is trap-assisted tunneling (TAT),[2] which can happen between a trap and a contact (Si-substrate or gate electrode materials), or between one trap and another one if the density of traps is very high. Recent experimental results indicate that the hole trapping is one of reasons causing the negative bias and temperature instability (NBTI) for a p-channel MOS field effect transistor (P-MOSFET) and is proposed as a multiphonon (MP) process.[3] Random telegraph signals in the drain current of a MOSFET are due to carrier capture and emission from a trap in a gate dielectric.[4] So it is important to understand the mechanisms of the trap-related carrier capture and emission.

Besides a lot of phenomenological models, there are three basic microscopic mechanisms for TAT in the literature. Lundstrom *et al.*[5] proposed a model for an electron to tunnel from Si to into a deep neutral trap with a three dimensional (3D) δ-function potential well using Bardeen's transfer Hamiltonian method.[6] The matrix element of the tunneling transition is $\int F_s(r)V_\delta F_t(r)d^3r = \langle F_s|V_\delta|F_t\rangle$. Here $F_s(r)$ is the effective-mass envelope wave function of a Si conduction band electron whose tail tunnels into SiO_2; V_δ and $F_t(r)$ are the short-ranged trap potential and the envelope wave function of the trap ground state, respectively. The integration over $\vec{r}$ is limited to a small volume around the trap due to the short-ranged nature of V_δ. Vuilaume *et al.* gave a similar model for an electron to tunnel from Si substrate into a deep neutral trap with a 3D spherical potential well.[7] In these two models, the short-ranged potential generated by the trap is the interaction causing the electron capture transition. Price and Sah used a similar idea for the field ionization of an electron from a trap in a solid in a high electric field.[8] The transition matrix element of the field ionization is proportional to $\int F_o(r)V_\delta F_t(r)d^3r = \langle F_o|V_\delta|F_t\rangle$, where $F_o(r)$ is the effective-mass wave function of a continuum state in SiO_2 conduction band in an electric field.[8] The effect of the MP emission or absorption on the field-induced tunneling ionization has been treated by Karpus *et al.* based on a quasiclassical approximation[9,10] and by Makram-Ebeid and Lannoo based on a full quantum theory.[11] As the wave functions of the quantum defect model have taken into account the effect of the core charge of a trap, the Makram-Ebeid-Lannoo model can deal with both neutral and charged traps. Nasyrov *et al.* have used this model to study the trap-assisted charge injection in a silicon-oxide–nitride-oxide-silicon (SONOS) structure.[12] We will call this trap potential induced transition mechanism 1 (M1) in the following sections.

For an electron to emit out from a trap in an electric field, the interaction in the transition element is the short-ranged trap potential in the Price-Sah model,[8] which is the same as that used by Lundstrom *et al.* for an electron capture process. In comparison, the perturbing interaction is the electric field in the Makram-Ebeid-Lannoo model, in which the transition matrix element is proportional to $\int F_o(r)qF_{ox}zF_t(r)d^3r = \langle F_o|qF_{ox}z|F_t\rangle$, where q is the electron charge, and F_{ox} and z are the electric field and the coordinate in the z direction in the oxide, respectively. The two models seem very different. Do they give different predictions? Later we will prove that $\langle F_o|qF_{ox}z|F_t\rangle$ is only approximately right.

In solids, electronic and nuclear freedoms can be separated by using Born-Oppenheimer's adiabatic approximation. The remaining nonadiabatic interaction part can cause MP

[a]Electronic mail: zhangmanhong@ime.ac.cn.

 © 2011 American Institute of Physics

Downloaded 05 Sep 2013 to 35.8.11.2. This article is copyrighted as indicated in the abstract. Reuse of AIP content is subject to the terms at: http://jap.aip.org/about/rights_and_permissions

radiationless transitions during electron capture or emission and has been studied by many authors.[13,14] Using the MP transitions based on the nonadiabatic interaction, Jimenez-Molinos *et al*. have studied TAT and random telegraph signals in metal-oxide-semiconductor (MOS) structures.[15,16] We call this nonadiabatic interaction induced transition mechanism 2 (M2) in the following sections. In the calculation of transition rates in mechanisms 1 and 2, the effective mass approximation is usually used. The wave function of an electron state can be written as $\psi(\vec{r}) = F(\vec{r})u(\vec{r})$, where $F(\vec{r})$ is the envelope function and $u(\vec{r})$ is the periodic Bloch function in a primitive cell. It is also assumed that $u(\vec{r})$ is the same for an electron in Si and SiO_2 conduction bands and in the trap state in SiO_2. Although it is a very crude approximation, published calculations based on this assumption in the literature still give satisfactory agreement with experimental results.

Schenk *et al*.[17] proposed another trap-to-band transition mechanism by assuming $u(\vec{r}) = u_c(\vec{r})$ for an electron initially in Si conduction band and $u(\vec{r}) = u_v(\vec{r})$ for the trap state in a deep trap in SiO_2. Here $u_c(\vec{r})$ and $u_v(\vec{r})$ are Bloch functions of the bottom of the conduction band and the top of the valence band of SiO_2, respectively. As $\int_\Omega u_c(\vec{r})u_v(\vec{r})d^3r = 0$ in a volume of a primitive cell, the rate of MP transition based on this mechanism is totally different from the other mechanisms mentioned above. The transition matrix element in Schenk's model is $\langle F_s|F_t\rangle \int_\Omega u_c(\vec{r})qF_{ox}zu_c(\vec{r})d^3r \doteq \langle F_s|F_t\rangle\langle u_c|qF_{ox}z|u_v\rangle$. Here Ω is the volume of a primitive cell and $F_t(r)$ is the envelope function for the trap ground state, which for a deep neutral trap can be approximated by Lucovsky's wave function, $\sqrt{(\kappa/2\pi)}\exp(-\kappa r)/r$.[18] It is an electric field induced trap−band transition mechanism similar to the Zener band−band transition in a bulk semiconductor. Schenk *et al*. gave a detailed implementation of this mechanism and used it to study the TAT in SiO_2.[19] Many authors have used it to extract trap properties such as Refs. 20 and 21. However, after a careful examination of Ref. 19 one can find some drawbacks in some of its equations. The electron concentration in the Si conduction band in the cathode was described by a bulk density of states using a parabolic band approximation with the total electron kinetic energy as an integral argument. The electron tunnel probability in SiO_2 was calculated using Wentzel-Kramers-Brillouin (WKB) approximation. However, it is the total electron energy (including kinetic energy components in both the perpendicular and in-plane movements) of the incident electron that was used to calculate the tunnel probability in Ref. 19. Such an approximation does not agree with the conclusions of Refs. 2 and 22 where it has been shown that the tunnel probability is mainly determined by the perpendicular kinetic energy of the initial electron and very weakly depends on the in-plane kinetic energy. In addition, other approximations adopted in Ref. 19 are setting the preexponential factor of the tunneling probability to 1 and using a 1D tunneling formula for the 3D field ionization of a trapped electron through a triangle barrier into the SiO_2 conduction band. We call this field-induced transition mechanism 3 (or Schenk's model) in the following sections.

The above three mechanisms for the MP TAT processes have very different physics. However, most papers just pick up one mechanism to explain their data. The goal of the present paper is to compare all three mechanisms. We will correct the drawbacks in Schenk's model. For a NMOS structure under a negative gate bias, we include electron capture from a poly-Si cathode and its reverse process: electron emission back to the poly-Si cathode, electron emission to the Si-substrate, and most important, electron emission to SiO_2 through the field ionization. The last process is critical in the Fowler-Nordheim (FN) injection region. The trap-to-trap tunneling process may be important in some cases.[23] We ignore it in the present investigation for simplicity.

II. TRANSITION RATES UNDER THE ZERO-PHONON CASE

A. Transition rate induced by the short-ranged trap potential

In order to study the tunnel ionization in an electric field, the wave function of conduction band states of SiO_2 under a high electric field is needed. An unpenetrating barrier wall is imposed to discretize the continuum spectra (see Fig. 1). The area A in the x-y plane and the length L in the field direction (z direction) are assumed large enough. The envelope wave function is

$$F_o(r) = \sqrt{\frac{1}{A}}\exp(i\vec{k}_{||}\bullet\vec{\rho}) \times \frac{\sqrt{\pi}}{(Ll)^{1/4}}Ai(-\xi) \equiv \phi(\vec{k}_{||},\vec{\rho})f_o(z), \tag{1}$$

where $\xi = (z/l) + \lambda$, $l = (2m_{ox}qF_{ox}/\hbar^2)^{1/3}$, and $\lambda/l^2 = 2m_{ox}(E_z - \varphi_0)/\hbar^2$.[2] The definitions $\phi(\vec{k}_{||},\vec{\rho}) \equiv \sqrt{(1/A)}\exp(i\vec{k}_{||}\bullet\vec{\rho})$ and $f_o(z)$ are also introduced for later use. The plane wave $\phi(\vec{k}_{||},\vec{\rho})$ describes the movement in the x-y plane. The electron potential energy is φ_0-$qF_{ox}z$ with $\varphi_0 = 3.15$ eV as the conduction band offset between Si and SiO_2 and F_{ox} as the oxide electric field. $z = 0$ is at the poly-Si/SiO_2 interface. The energy eigenvalue for the movement in the z direction is determined by requiring $f_o(L) = 0$. Using the asymptotic expansion for Airy function $Ai(-\xi)$ for $\xi \gg 0$, we have

$$F_o(r) = \phi(\vec{k}_{||},\vec{\rho})\frac{\sqrt{\pi}}{(Ll)^{1/4}}\frac{1}{\sqrt{\pi}\xi^{1/4}}\sin\left(\frac{2}{3}\xi^{2/3} + \frac{\pi}{4}\right). \tag{2}$$

Setting $2/3(L/l + \lambda)^{3/2} + \pi/4 = n\pi$ with n as an integer, the eigenvalues of E_z can be determined. The above envelop function is properly normalized in the box of $A \times L$. The density of states due to the quantization in the z direction is

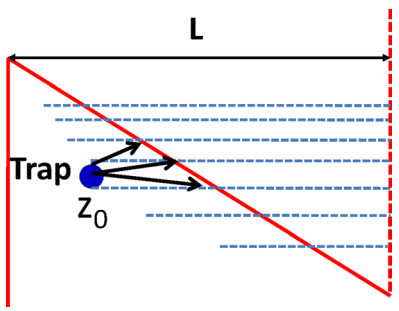

FIG. 1. (Color online) Discretization of the continuum conduction band states of SiO_2 in a high electric field using an unpenetrating barrier wall at $z = L$. A trap is located at $z = z_0$.

Downloaded 05 Sep 2013 to 35.8.11.2. This article is copyrighted as indicated in the abstract. Reuse of AIP content is subject to the terms at: http://jap.aip.org/about/rights_and_permissions

$dn/dE_z = 2m_{ox}\sqrt{Ll^3}/(\pi\hbar^2)$, where no spin-summation is needed.

In order to simplify the calculation, we will only consider deep neutral traps. A neutral trap generates a very short and strong potential perturbation to the bulk crystal. This short-ranged potential can be simulated by a spherical potential well with a radius of r_a and a depth of V_0. Outside of the potential well, the influence of the trap is set to zero and the envelope wave function has a form of $\exp(-\kappa r)/r$ with a trap energy of $E_t = -(\hbar^2\kappa^2/2m_{ox})$. At the limit of 3D δ-function potential well by letting $r_a \to 0$, $r_a\kappa \to 0$, $V_0 r_a^2 \to (\hbar^2/2m_{ox})(\pi/2)^2$,[7] the whole envelope wave function of the trap can be approximated as

$$F_t(r) = \sqrt{\frac{\kappa}{2\pi}}\exp(-\kappa r)/r. \tag{3}$$

It is the so-called Lucovsky's wave function. The short-ranged potential of the trap can be approximated by a pseudopotential of $V_\delta(\vec{r}) = 4\pi E_t r_t^3 \delta(\vec{r})(1 + \vec{r}\bullet\nabla)$ in this limit. The trap energy is still $E_t = -(\hbar^2\kappa^2/2m_{ox})$ and the trap radius becomes $r_t = 1/\kappa$. The condition of $qF_{ox}r_t \ll V_0$ is assumed so that the effect of F_{ox} on the $F_t(r)$ can be ignored.

Let us first explain the difference in the transition matrix elements for the tunneling ionization between the Price-Sah and Makram-Ebeid-Lannoo model. With the assumption of the same periodic Bloch function part of $u_c(r)$ for the conduction band state and the trap sate, the following transition matrix element for the zero-phonon tunneling ionization can be obtained as demonstrated by the Price-Sah model:

$$\begin{aligned}&\int_{|\vec{r}-\vec{r}_0|<r_a} F_o(\vec{r})V_0(\vec{r}-\vec{r}_0)F_t(\vec{r}-\vec{r}_0)d^3r \\ &\quad\xrightarrow{r_a\to 0}\int_{\text{allspace}} F_o(\vec{r})V_0(\vec{r}-\vec{r}_0)F_t(\vec{r}-\vec{r}_0)d^3r, \\ &\quad= \langle F_O|V_\delta|F_t\rangle.\end{aligned} \tag{4}$$

Here the deep neutral trap is located at the point of $\mathbf{r_0}$. The effect of the oxide electric field is fully included in $F_o(\vec{r})$. In above equation, the transition matrix is written by considering the short ranged trap potential of $V_0(\vec{r}-\vec{r}_0)$ as a perturbation to the SiO_2 conduction band states. Based on Bardeen's transfer Hamiltonian method, it also can be written by taking the electric field-induced potential $qF_{ox}(z-z_0)$ as a perturbation to the trap state $F_t(\vec{r}-\vec{r}_0)$, so one also has the transition matrix element for the zero-phonon tunneling ionization:

$$\begin{aligned}&\int_{|\vec{r}-\vec{r}_0|>r_a} F_o(\vec{r})qF_{ox}(z-z_0)F_t(\vec{r}-\vec{r}_0)d^3r \\ &\quad\xrightarrow{r_a\to 0}\int_{\text{allspace}} F_o(\vec{r})qF_{ox}(z-z_0)F_t(\vec{r}-\vec{r}_0)d^3r \\ &\quad= \langle F_O|qF_{ox}(z-z_0)|F_t\rangle.\end{aligned} \tag{5}$$

The equivalence between Eqs. (4) and (5) should be approximate as the transfer Hamiltonian method is the first order perturbation theory. A simple calculation based on tunneling into the state of a δ-well inside a one dimension barrier proves the transition matrix in two approaches are only of the same order, but not exactly equal to each other.

Using Eq. (4) and Fermi golden rule one can easily calculate the zero-phonon tunneling ionization rate under an electric field as

$$\begin{aligned}W_{t,o} &= \sum_{k_{||}}\sum_n \frac{2\pi}{\hbar}|\langle F_o|V_\delta|F_t\rangle|^2\delta(E_o(k_{||},n) + qF_{ox}z_0 + E_t) \\ &= \sum_{k_{||}}\frac{2\pi}{\hbar}|\langle F_o|V_\delta|F_t\rangle|^2\frac{dn}{dE_z} \\ &= \frac{r_t qF_{ox}}{2\hbar}\exp\left(-\frac{4}{3}\frac{\sqrt{2m_{ox}}}{\hbar qF_{ox}}|E_t|^{3/2}\right).\end{aligned} \tag{6}$$

The energy eigenvalue of an electron in the SiO_2 conduction band with an unpenetrating wall at $z = L$ is

$$\begin{aligned}E_o(k_{||},n) &\equiv E_z + \frac{\hbar^2}{2m_{ox}}k_{||}^2 = \left(-qF_{ox}z + \frac{\hbar^2}{2m_{ox}}k_z^2\right) + \frac{\hbar^2}{2m_{ox}}k_{||}^2 \\ &= -qF_{ox}L + \frac{\hbar^2}{2m_{ox}}\left[k_{||}^2 + k_z(L)^2\right].\end{aligned} \tag{7}$$

Here $k_z(L)$ is determined by the above quantization condition. The calculated value of $W_{t,o}$ is exactly the same as the result for the 3D δ -function trap in the text book.[11] The capture process induced by the short-ranged potential of a deep trap has been calculated by Lundstrom *et al.*[5] Here we extend their calculation by including six-valleys of Si conduction bands and further taking account of the effective mass discontinuity in Si and SiO_2. Assuming for a MOS structure with a poly-Si gate in $z < 0$, a layer of SiO_2 in the range of $0 < z < L$ and a p-type Si-substrate in $z > L$, and a negative gate bias so that electrons are emitted from the poly-Si gate, according to Ref. 23 the wave function of an electron state in the poly-Si conduction band is

$$\begin{aligned}F_{s1}(\vec{r}) &= \phi(\vec{k_{||}},\vec{\rho})f_{s1}(z) \\ &= \phi(\vec{k_{||}},\vec{\rho})\sqrt{\frac{2}{L_{s1}}}\cos(k_{1z}z + \Delta_1) \quad \text{for } (z < 0), \\ &= \phi(\vec{k_{||}},\vec{\rho})\sqrt{\frac{2}{L_{s1}}}\frac{B_1}{\kappa(z)} \\ &\quad\times\exp\left(-\int_0^z \kappa(z')dz'\right) \quad \text{for } (0 < z < L).\end{aligned} \tag{8}$$

Here F_{s1} is normalized in a box of $A \times L_{S1}$ and $\kappa(z)$ is the imaginary wave number inside SiO_2. Its energy eigenvalue is $E_{s1}(\vec{k_{||}},k_{s1z}) = (\hbar^2/2m_{s1\perp})k_{||}^2 + (\hbar^2/2m_{s1z})k_{s1z}^2$ in the poly-Si gate. Considering the energy conservation during an electron capture, one has

$$E_{s1}(\vec{k_{||}},k_{s1z}) = \varphi_0 - qF_{ox}z + \frac{\hbar^2}{2m_{ox}}k_{||}^2 - \frac{\hbar^2}{2m_{ox}}k(z)^2, \tag{9a}$$

$$= \varphi_0 - qF_{ox}z_0 - |E_t|. \tag{9b}$$

$$\kappa(z) = \sqrt{\frac{2m_{ox}}{\hbar^2}[qF_{ox}(z_0 - z) + |E_t|] + k_{||}^2}. \tag{10}$$

The parameter B_1 is determined from the wave function matching at $z = 0$ with an abrupt potential boundary:

Downloaded 05 Sep 2013 to 35.8.11.2. This article is copyrighted as indicated in the abstract. Reuse of AIP content is subject to the terms at: http://jap.aip.org/about/rights_and_permissions

$$B_1 = \left[\frac{1}{\kappa(0)} + \frac{\kappa(0)m_{s1z}}{k_{s1z}^2 m_{ox}}\right]^{-1/2}. \quad (11)$$

The above equations for F_{s1} are taken from Ref. 22 with some minor definition changes. The quantity m_{s1z} is the effective mass of a conduction band valley in z direction in poly-Si (S1). Similarly, the wave function of electron states in Si-substrate (S2) can be built, too. For an electron to be captured by a deep neutral trap at z_0, the zero-phonon tunneling capture rate is

$$\begin{aligned}
W_{s1,t} &= \sum_{\nu}\sum_{k||}\sum_{k_{s1z}} \frac{2\pi}{\hbar}|\langle F_{s1}|V_\delta|F_t\rangle|^2 f_{FD}(\vec{k}_{||}, k_{s1z}) \\
&\quad \times \delta(E_{s1}((\vec{k}_{||}, k_{s1z}) - \varphi_0 + qF_{ox}z_0 + |E_t|) \\
&= \sum_{\nu}\sum_{k||} \frac{2\pi}{\hbar}|\langle F_{s1}|V_\delta|F_t\rangle|^2 f_{FD}(\vec{k}_{||}, k_{s1z})\rho_{s1z} \\
&= \sum_{\nu}\sum_{k||} \frac{2\pi}{\hbar}|\langle F_{s1}|V_\delta|F_t\rangle|^2 f_{FD}(\vec{k}_{||}, k_{s1z})\frac{2L_{s1}m_{s1z}}{\pi k_{s1z}\hbar^2} \\
&= \sum_{\nu}\frac{8\hbar m_{s1z}}{r_t m_{ox}^2}\int_0^{+\infty} dk_{||}k_{||}\frac{\kappa(0)}{\kappa(z_0)}\frac{k_{s1z}f_{FD}(\vec{k}_{||}, k_{s1z})}{\left[k_{s1z}^2 + \kappa(0)^2 m_{s1z}^2/m_{ox}^2\right]} \\
&\quad \times \exp[-2S(z_0)]. \\
&\approx \sum_{\nu}\frac{8\hbar m_{s1z}}{r_t m_{ox}^2}\int_0^{+\infty} dk_{||}k_{||}\frac{\kappa(0)}{\kappa(z_0)}\frac{k_{s1z}f_{FD}(\vec{k}_{||}, k_{s1z})}{\left[k_{s1z}^2 + \kappa(0)^2 m_{s1z}^2/m_{ox}^2\right]} \\
&\quad \times \exp(-k_{||}^2 z_0 r_t)\exp[-2S'(z_0)]. \quad (12)
\end{aligned}$$

Here $\rho_{s1z} = (2L_{s1}m_{s1z})/(\pi k_{s1z}\hbar^2)$ is the density of states per unit-energy interval in z direction for incident electrons in the poly-Si gate including a factor of 2 for the spin summation. The summation v refers to six valleys of Si conduction bands. $f_{FD}(\vec{k}_{||}, k_{s1z})$ is the Fermi-Dirac occupation numbers of electrons in each valley of poly-Si conduction bands. Usually a deep neutral trap can take only one electron in the ground state, so incident electrons with two different spins have chances to be captured into one empty trap and the emitted electron from a filled trap has only one kind of spin. The final results can be calculated by changing the summation over $\vec{k}_{||}$ into an integral. The expression is very similar to that obtained by Lundstrom *et al.*[5] The factor $S(z_0)$ or $S'(z_0)$ include the effect of the oxide electric field on $W_{s1,t}$, which are defined by

$$\begin{aligned}
S(z_0) &= \frac{2\sqrt{2m_{ox}}}{3\hbar qF_{ox}}\left[\left(qF_{ox}z_0 + \frac{\hbar^2}{2m_{ox}}k_{||}^2 + |E_t|\right)^{3/2}\right. \\
&\quad \left. -\left(\frac{\hbar^2}{2m_{ox}}k_{||}^2 + |E_t|\right)^{3/2}\right], \quad (13a) \\
&\approx \frac{2\sqrt{2m_{ox}}}{3\hbar qF_{ox}}\left[(qF_{ox}z_0 + |E_t|)^{3/2} - |E_t|^{3/2}\right] + \frac{1}{2}k_{||}^2 z_0 r_t, \quad (13b) \\
&\equiv S'(z_0) + \frac{1}{2}k_{||}^2 z_0 r_t. \quad (13c)
\end{aligned}$$

The above Taylor expansion approximation is valid for large $|E_t|$ with respect to terms of $qF_{ox}z_0$ and $(\hbar^2/2m_{ox})k_{||}^2$. A detailed numerical computation indeed shows that $S(z_0)$ weakly depends on $k_{||}$. It is also possible for a trapped electron to emit back to S1, the corresponding rate $W_{t,s1}$ is obtained by changing $f_{FD}(\vec{k}_{||}, k_{s1z})$ into $[1 - f_{FD}(\vec{k}_{||}, k_{s1z})]$. For the process of a trapped electron to tunnel out to the Si-substrate (S2), it is also straightforward to calculate the transition rate using a wave function similar to Eq. (8).[22] For the convenience, this transition rate is denoted as $W_{t,s2}$ in the following section.

B. Transition rate in mechanism 3

In mechanism 3 (Schenk's model), the cell periodic Bloch function parts for the conduction band states and the trap state are $u_c(r)$ and $u_v(r)$, respectively. So our transition rate of tunnel ionization to SiO_2 can be written as

$$\begin{aligned}
W_{t,o} &= \sum_{k_{||}}\sum_{n}\frac{2\pi}{\hbar}\left[\langle F_o|F_t\rangle\int_\Omega u_c(\vec{r})qF_{ox}zu_v(\vec{r})d^3r\right]^2 \\
&\quad \times \delta(E(k_{||}, n) + qF_{ox}z_0 + |E_t|), \\
&= \sum_{k_{||}}\frac{2\pi}{\hbar}\left[\langle F_o|F_t\rangle\int_\Omega u_c(\vec{r})qF_{ox}zu_v(\vec{r})d^3r\right]^2\frac{dn}{dE_z}, \\
&\approx \frac{2m_{ox}^2 r_t^5 qF_{ox}}{\hbar^5}(qF_{ox}x_{ct})^2\exp\left(-\frac{4}{3}\frac{\sqrt{2m_{ox}}}{\hbar qF_{ox}}|E_t|^{3/2}\right). \quad (14)
\end{aligned}$$

Here $x_{ct} \equiv \int_\Omega u_c(\vec{r})zu_v(\vec{r})d^3r = (\hbar/\sqrt{2m_{ox}E_{go}}$ is defined with E_{go} for the bandgap of SiO_2 according to Schenk.[17] Similarly, the transition rate for an electron from poly-Si (S1) to a trap is

$$\begin{aligned}
W_{s1,t} &= \sum_{\nu}\sum_{k||}\sum_{k_{s1z}}\frac{2\pi}{\hbar}\left[\langle F_o|F_t\rangle\int_\Omega u_c(\vec{r})qF_{ox}zu_v(\vec{r})d^3r\right]^2 \\
&\quad \times f_{FD}(\vec{k}_{||}, k_{s1z})\delta(E_{s1}((\vec{k}_{||}, k_{s1z}) - \varphi_0 + qF_{ox}z_0 + E_t), \\
&= \sum_{\nu}\sum_{k||}\frac{2\pi}{\hbar}\left[\langle F_o|F_t\rangle\int_\Omega u_c(\vec{r})qF_{ox}zu_v(\vec{r})d^3r\right]^2 \\
&\quad \times f_{FD}(\vec{k}_{||}, k_{s1z})\rho_{s1z}, = \sum_{\nu}\frac{16r_t^3 m_{s1z}}{\hbar^3} \\
&\quad \times \int_0^{+\infty} dk_{||}k_{||}\frac{\kappa(0)}{\kappa(z_0)}\frac{k_{s1z}\exp(-k_{||}^2 z_0 r_t)f_{FD}(\vec{k}_{||}, k_{s1z})}{\left[k_{s1z}^2 + \kappa(0)^2 m_{s1z}^2/m_{ox}^2\right]} \\
&\quad \times \exp[-2S'(z_0)]. \quad (15)
\end{aligned}$$

Here $\kappa(z)$ and $S'(z_0)$ have the same definitions as those in Eq. (10) and Eq. (13c), respectively. $\exp[-2S'(z_0)]$ is the tunnel probability from poly-Si to z_0 in SiO_2.[17] Similar equations can be derived for the transition rates of $W_{t,s1}$ and $W_{t,s2}$ based on the idea of Schenk's model.[17] These equations are different from those old ones in Ref. 17 due to using the correct tunnel probability of the incident electron and the properly box-normalized wave function [Eq. (1)] for a conduction band state in SiO_2 under a high electric field.

III. TRANSITION RATES UNDER THE MULTIPHONON CASE

A. The electron−phonon basis under adiabatic approximation

To separate the fast electron freedom and the slow nuclear movement, the adiabatic Born-Oppenheimer approximation is

Downloaded 05 Sep 2013 to 35.8.11.2. This article is copyrighted as indicated in the abstract. Reuse of AIP content is subject to the terms at: http://jap.aip.org/about/rights_and_permissions

usually used. In this approximation, the electron wave function is first solved for arbitrary fixed configuration of atoms by solving the following Schrödinger equation:

$$[T_r + V(r,R)]\psi_v(r,R) = E_v(R)\psi_v(r,R), \tag{16}$$

where r and R stand for the coordinates of the electron and the atoms, respectively. T_r, $V(r, R)$, and $\psi_v(r, R)$ are the kinetic, potential operators and the wave function of an electron. $E_v(R)$ is the energy of an electronic state denoted by quantum number v. The movement of atoms is then subjected to the following equation:

$$[\mathrm{T}_R + V(R) + E_v(R) + L_{vv} - \varepsilon]\Phi_v(R) = -\sum_{\mu}^{\prime} L_{v\mu}\Phi_\mu(R), \tag{17}$$

$$L_{v\mu} = -\frac{\hbar^2}{2M}\sum_i \left[\int \psi_\nu^*(r,R)\frac{\partial^2}{\partial R_i^2}\psi_\mu(r,R) + 2\int d^3r\psi_\nu^*(r,R)\frac{\partial}{\partial R_i}\psi_\mu(r,R)\frac{\partial}{\partial R_i}\right]. \tag{18}$$

Here T_R and $V(R)$ are the kinetic and inter-atom potential operators, respectively. Neglecting $L_{v\mu}$ in Eq. (17) decouples the electronic and vibrational subsystems (adiabatic approximation). Expanding the total potential to the second order in atom displacements (ΔR) as well, one solves Eq. (16) and obtains the vibrational spectra $\hbar\omega_\mu$ and the corresponding normal mode coordinates q_μ. The total wave function is written as $\psi_v(r,R)\prod_\mu \Phi_{n\mu}(q_\mu - q_{\mu 0}^v)$ in this approximation, where $\Phi_{n\mu}(q_\mu - q_{\mu 0}^v)$ is the wave function of the $n\mu$th excited state for a harmonic oscillator and $q_{\mu 0}^v$ is the equilibrium position of phonon mode μ in the electronic state v. The nonadiabatic interaction term, Eq. (16), may give rise to the radiationless MP transition between a state of $\psi_v(r,R)\prod_\mu \Phi_{n\mu}(q_\mu - q_{\mu 0}^v)$ and another state of $\psi_{v'}(r,R)\prod_{\mu'} \Phi_{n\mu'}(q_{\mu'} - q_{\mu' 0}^{v'})$.

For further calculation, we follow Makram-Ebeid and Lannoo by adopting an approximation of a single phonon mode and a linear electron−phonon coupling.[11] The linear electron−phonon coupling between the trapped electron and the phonon mode takes the following form

$$H_{eL} = -\sqrt{2S}Q\hbar\omega, \tag{19}$$

In which $\hbar\omega$ is the phonon energy, Q is the normal coordinate and S is the Huang-Rhys coupling constant. The phonon Hamiltonian is $H_L = -(\hbar\omega/2)(d^2/dQ^2) + (\hbar\omega/2)Q^2$. The coupling H_{eL} makes the trap state and the lattice vibration behave as a harmonic oscillator with the equilibrium position of Q shifted by $\sqrt{2S}$. Writing the total wave function and the total energy of trap electronic state and phonon state as

$$\Psi_t(r,Q) = \psi_t(r,Q)\Phi_{nt}(Q - \sqrt{2S}), \tag{20}$$

$$E_{tL} = E_{t0} + H_{eL} + H_L = (E_{t0} - S\hbar\omega) - \frac{\hbar\omega}{2}\frac{d^2}{dQ^2} + \frac{\hbar\omega}{2}(Q - \sqrt{2S})^2 = E_t + \hbar\omega\left(n_t + \frac{1}{2}\right). \tag{21}$$

Here E_{t0} and $E_t = E_{t0} - S\hbar\omega$ are the bare and renormalized trap energy, respectively. $E_t(Q) \equiv E_t + S\hbar\omega - \sqrt{2S}\hbar\omega Q$ has an explicit dependence on Q and corresponds to $E_v(R)$ in Eq. (14). From the text book of Ridley,[24] it is reasonable to assume that the averaged electron−phonon coupling between the extending electron states and the phonon mode is small, so the equilibrium position change of the oscillator in an extending electronic state is negligible. The composite wave-function of the extending electronic state and the lattice vibration is

$$\Psi_e(r,Q) = \psi_e(r,Q)\Phi_{ne}(Q), \tag{22}$$

$$E_{eL} \approx E_{e0} + H_L = E_{e0} - \frac{\hbar\omega}{2}\frac{d^2}{dQ^2} + \frac{\hbar\omega}{2}Q^2 = E_e + \hbar\omega\left(ne + \frac{1}{2}\right). \tag{23}$$

The electron−phonon interaction does not change the energy of the extending electronic state ($E_e = E_{e0}$). Figure 2 shows schematically the energies of both extending and trap state on Q in a configuration coordinate.

For the emission of an electron from a trap state to an extending state, the energy conservation requires that $E_t - E_e = (ne - nt)\hbar\omega \equiv p\hbar\omega$, and the transition rate is

$$W = \frac{2\pi}{\hbar}Av_{nt}\sum_{ne}|\langle\Psi_e(r,Q)|H'|\Psi_t(r,Q)\rangle|^2 \times \delta(E_e - E_t + p\hbar\omega). \tag{24}$$

Here the perturbation interaction H' can be the short-ranged trap potential in mechanism 1, or $qF_{\mathrm{ox}}z$ in Schenk's model, or the nonadiabatic interaction H_{NA}, which corresponds to $L_{v\mu}$ in Eq. (17). The symbol Av_{nt} stands for the statistical average over the initial vibration state.

B. MP transition rates in mechanism 1 and 3

When the perturbation interaction H' is the trap potential in mechanism 1, or $qF_{\mathrm{ox}}z$ in mechanism 3, the transition rate can be calculated by

$$W = \frac{2\pi}{\hbar}Av_{nt}\sum_{ne}|\langle\psi_e(r,Q=0)|H'|\psi_t(r,Q=Q_t)\rangle|^2 \times |\langle\Phi_{nt+p}(Q)|\Phi_{nt}(Q - \sqrt{2S})\rangle|^2\delta(E_e - E_t + p\hbar\omega). \tag{25}$$

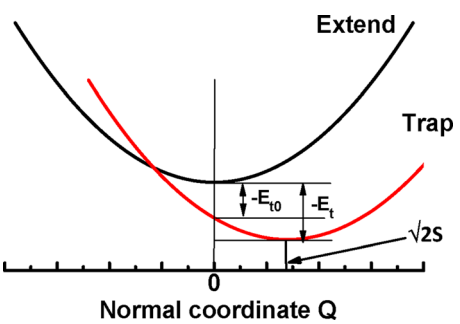

FIG. 2. (Color online) The schematic diagram for the dependence of the energies of extending and trap state on the normal coordinates Q. Parameter E_{t0}, E_t, and $\sqrt{2S}$ are defined in Eq. (21).

Downloaded 05 Sep 2013 to 35.8.11.2. This article is copyrighted as indicated in the abstract. Reuse of AIP content is subject to the terms at: http://jap.aip.org/about/rights_and_permissions

In the matrix element $\langle\psi_e(r,Q=0)|H'|\psi_t(r,Q=Q_t)\rangle$, Q_t is evaluated at $E_t(Q_t)=E_e$ by following argument of Makram-Ebeid and Lannoo.[11]

$$\begin{aligned}W &= \frac{2\pi}{\hbar}Av_{nt}\sum_{ne}|\langle\psi_e(r,Q=0)|H'|\psi_t(r,Q=Q_t)\rangle|^2\\ &\quad\times|\langle\Phi_p(Q)|\Phi_{nt}(Q-\sqrt{2S})\rangle|^2\delta(E_e-E_t+p\hbar\omega),\\ &= \frac{2\pi}{\hbar}\sum_{p}|\langle\psi_e(r,Q=0)|H'|\psi_t(r,Q=Q_t)\rangle|^2\\ &\quad\times W_p^c\delta(E_e-E_t+p\hbar\omega).\end{aligned}\tag{26}$$

Here W_p^c is the so-called the line shape factor[11] and defined through

$$\begin{aligned}W_p^c &= Av_{nt}|\langle\Phi_{nt+p}(Q)|\Phi_{nt}(Q-\sqrt{2S})\rangle|^2\\ &= \exp\left(\frac{p\hbar\omega}{2kT}-S\coth\left(\frac{\hbar\omega}{2kT}\right)\right)\mathrm{I}_p\left[\frac{S}{\sinh(\hbar\omega/2kT)}\right].\end{aligned}\tag{27}$$

Here $I_p(x)$ is the modified Bessel function of the order p. For the emission rate, another summation is also assumed over the final extending electronic states in Eq. (26). To calculate the capture rate from an extending electronic state, the statistical average should be performed over the initial vibration state using Av_{ne} and p in Eq. (27) should be replaced by $p'\equiv nt-ne=-p$. The final MP transition rates in mechanism 1 and 3 can be obtained by making a change of $E_t\rightarrow E_t+p\hbar\omega$ in the zero-phonon transition rates and timing the factor of W_p^c for the emission (or W_{-p}^c for the capture).

C. MP transition rates in mechanism 2

For the transition between the trap state and an extending electronic state induced by the nonadiabatic interaction H_{NA}, the transition rate is

$$W=\frac{2\pi^2}{\hbar}(S\hbar\omega)^2\frac{V_t}{A}f(z_0)^2\left(1-\frac{p}{S}\right)^2W_p^c\delta(E_i-E_f-p\hbar\omega).\tag{28}$$

Here E_i and E_f stand for the electronic energies of initial and final states, respectively. The z coordinate of the trap is at z_0. $V_t=4\pi r_t^3/3$ is the trap volume. $f(z)$ is the envelope wave function of the extending electronic state in z direction. Other parameters have the same meaning as above. To get the total transition rate, a summation over the density of states of the extending electronic states is also needed. For tunneling ionization, the transition rate is

$$\begin{aligned}W_{t,o} &= \frac{2\pi^2}{\hbar}\sum_p\sum_{k_{||},n}(S\hbar\omega)^2\frac{V_t}{A}f_o(z_0)^2\\ &\quad\times\left(1-\frac{p}{S}\right)^2W_p^c\delta(E(k_{||},n)+qF_{\mathrm{ox}}z_0+|E_t|-p\hbar\omega)\\ &= \frac{2\pi^2}{\hbar}\sum_p\sum_{k_{||}}(S\hbar\omega)^2\frac{V_t}{A}f_o(z_0)^2\left(1-\frac{p}{S}\right)^2W_p^c\frac{dn}{dE_z}\\ &= \frac{8\pi m_{\mathrm{ox}}^2r_t^5qF_{\mathrm{ox}}}{3\hbar^5}\sum_p(S\hbar\omega)^2\left(1-\frac{p}{S}\right)^2W_p^c\\ &\quad\times\exp\left(-\frac{4}{3}\frac{\sqrt{2m_{\mathrm{ox}}}}{\hbar qF_{\mathrm{ox}}}|E_t|^{3/2}\right).\end{aligned}\tag{29}$$

For an electron captured by the trap from poly-Si (S1), the transition rate is

$$\begin{aligned}W_{s1,t} &= \frac{2\times2\pi^2}{\hbar}\sum_{v,p}\sum_{k_{||},k1z}\frac{V_t}{A}f_{s1}(z_0)^2f_{\mathrm{FD}}(\vec{k_{||}},k_{s1z})(S\hbar\omega)^2\\ &\quad\times\left(1+\frac{p}{S}\right)^2W_{-p}^c\delta(E_{s1}(k_{||},k_{1z})\\ &\quad-(\varphi_0-qF_{\mathrm{ox}}z_0-|E_t|)+p\hbar\omega)\\ &= \frac{2V_tL_{s1}}{\hbar^3}\sum_{v,p}\int_0^{+\infty}dk_{1z}m_{s1||}f_{s1}(z_0)^2f_{\mathrm{FD}}(\vec{k_{||}},k_{s1z})(S\hbar\omega)^2\\ &\quad\times\left(1+\frac{p}{S}\right)^2W_{-p}^c\\ &= \frac{8\pi r_t^3}{3\hbar^3}\sum_{v,p}\int_0^{+\infty}dk_{1z}\frac{2m_{s1||}B_1^2}{\kappa(z_0)}\\ &\quad\times\exp[-2S(z_0)]f_{\mathrm{FD}}(\vec{k_{||}},k_{s1z})\\ &\quad\times(S\hbar\omega)^2\left(1+\frac{p}{S}\right)^2W_{-p}^c.\end{aligned}\tag{30}$$

The emission rate from a trap to S1 is

$$\begin{aligned}W_{t,s1} &= \frac{2\pi^2}{\hbar}\sum_v\sum_{k_{||},k1z}\frac{V_t}{A}f_{s1}(z_0)^2(1-f_{\mathrm{FD}}(\vec{k_{||}},k_{s1z}))(S\hbar\omega)^2\\ &\quad\times\left(1-\frac{p}{S}\right)^2W_p^c\delta(E_{s1}(k_{||},k_{1z})\\ &\quad-(\varphi_0-qF_{\mathrm{ox}}z_0-|E_t|)+\mathrm{p}\hbar\omega)\\ &= \frac{4\pi r_t^3}{3\hbar^3}\sum_v\int_0^{+\infty}dk_{1z}\frac{2m_{s1||}B_1^2}{\kappa(z_0)}\exp[-2S(z_0)]\\ &\quad\times(1-f_{\mathrm{FD}}(\vec{k_{||}},k_{s1z}))(S\hbar\omega)^2\left(1-\frac{p}{S}\right)^2W_p^c.\end{aligned}\tag{31}$$

Jimenez-Molinos *et al.* have calculated the transition rates using this mechanism, but they did not include the tunneling ionization from a trap to the SiO_2 conduction band.[15,16] In addition, they made further approximation over the summation of the density of states for the extending states to avoid complicated numerical computation. In this paper, we perform the integration in Eqs. (30) and (31) numerically.

IV. CALCULATION OF TAT-INDUCED GATE CURRENT

Assuming a bulk trap density of $N_t(z)$ in the SiO_2 layer with thickness L_o. The occupied trap density is $N_t(z)\times f(z)$, where $f(z)$ is the occupation number at the coordinate z. The change of $f(z)$ due to TAT is

$$\frac{df(z)}{dz}=W_{s1,t}[1-f(z)]-(W_{t,s1}+W_{t,s2}+W_{t,o})f(z).\tag{32}$$

Here tunneling between two traps are ignored. At a steady state, the value of $f(z)$ is

$$f_0(z)=W_{s1,t}/(W_{s1,t}+W_{t,s1}+W_{t,s2}+W_{t,o}).\tag{33}$$

The total TAT-induced gate current density can be calculated from the following equation:

$$J_{\mathrm{TAT}}=q\int_0^{Lo}dzN_t(z)(W_{t,o}+W_{t,s2})f_0(z)\equiv\int_0^{Lo}dzG_{\mathrm{bulk}}(z).\tag{34}$$

Here $G_{\mathrm{bulk}}(z)$ is the bulk current generation rate.

Downloaded 05 Sep 2013 to 35.8.11.2. This article is copyrighted as indicated in the abstract. Reuse of AIP content is subject to the terms at: http://jap.aip.org/about/rights_and_permissions

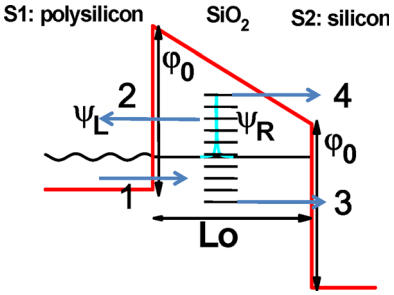

FIG. 3. (Color online) Four capture/emission processes included in the calculation: 1 for capture from poly-Si (S1), and 2 for emission to S1, 3 for emission to Si-substrate (S2), and 4 for emission to oxide.

Figure 3 shows schematically four transition processes: capture from poly-Si (S1), and emission to S1, to Si-substrate, and to oxide. To compare the differences between three mechanisms, we have calculated the TAT current based on the experimental data of Ref. 1 in which an NMOS capacitor with a 5.5 nm SiO_2 was stressed at a constant current stress of $J_g = -0.1$ A/cm^2 for 1 s. The voltage across the oxide layer can be calculated from $V_{ox} = V_g + 1.2$ V if $V_g < -1.2$ V. Gehring *et al.*[20] have simulated this experimental SILC using Schenk's model.[19] Their model parameters are $E_{t0} = -2.7$ eV, $S\hbar\omega = 1.3$ eV, and $N_t = 9.0 \times 10^{17}$ cm^{-3}.[20] However, the gate current they fitted is not purely SILC, but the total one including both the fresh gate current and SILC.[1] The SILC part was fitted using an empirical formula [Eq. (7)] in Ref. 1 so we calculate the TAT current using equations derived in this paper to compare with this fitting formula in Ref. 1 As the doping concentration of $n+$ poly-Si gate was not known, a reasonable value of 1×10^{20} cm^{-3} is used in our following calculation.

Our model parameters are $E_{t0} = -2.5$ eV, $S\hbar\omega = 1.2$ eV, and $N_t = 3.1 \times 10^{18}$ cm^{-3}. A uniform trap density gives a good fitting. Although Palma *et al.* found that the MP transition rates depend on the product of S and $\hbar\omega$,[16] we take two values (20 and 60 meV) of $\hbar\omega$ to test the sensitivity of results to parameters. The effective-mass values of Si and SiO_2 are taken from Ref. 22. Figure 4 shows J_{TAT} at 300 K in mechanism 1 and 2. It can be seen that J_{TAT} under two mechanisms are almost the same. In each mechanism, using

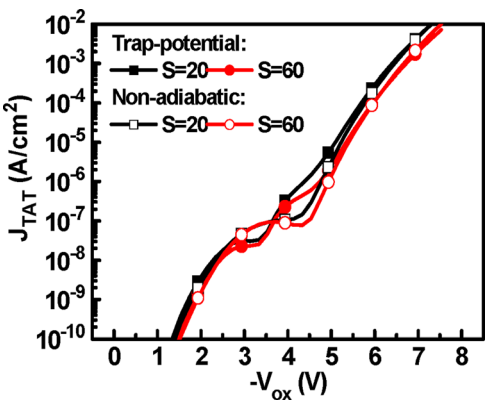

FIG. 4. (Color online) J_{TAT} at 300 K calculated using two MP transition mechanisms: the trap-potential induced transitions and the nonadiabatic interaction induced transitions. $S\hbar\omega$ is fixed at 1.2 eV.

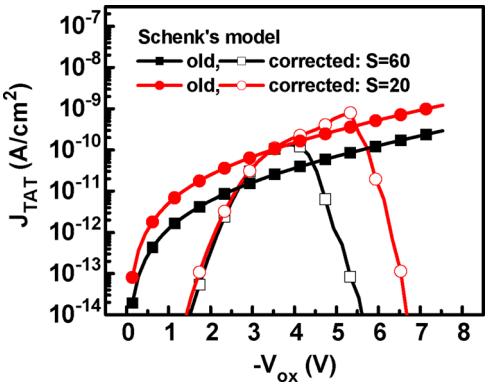

FIG. 5. (Color online) J_{TAT} at 300 K calculated using Schenk's model: the "old" data are calculated using equations in Ref. 19 and the "corrected" data are calculated using equations derived in this paper in mechanism 3.

$S = 20/\hbar\omega = 60$ meV gives rise to a larger J_{TAT} than using $S = 60/\hbar\omega = 20$ meV. Considering that there are some uncertainties of parameter values and approximation, two components of J_{TAT} should be in the same order.

Figure 5 shows J_{TAT} calculated using Schenk's model. The "old" data are calculated using equations in Ref. 19 and the "corrected" data are calculated using new equations derived in this paper. The corrected equations give a smaller J_{TAT} than the old equations in Ref. 19 at low and high V_{ox}. Comparing with Fig. 4, both the old and corrected equations give much smaller values of J_{TAT} in the Fowler-Nordheim region. So in the following calculation of total J_{TAT}, only mechanism 1 and 2 are considered. Figure 6 shows J_{SILC} from the fitting formula [Eq. (7) in Ref. 1] and our calculated total J_{TAT}. The experimentally measured J_{SILC} in Ref. 1 was in the range of $|V_{ox}| < 5.2$ V. The fitting formula makes it possible extrapolate to a larger range of V_{ox}. From Fig. 6, it is seen that choosing $S = 20/\hbar\omega = 60$ meV gives a better agreement between J_{TAT} and J_{SILC}. As mechanism 1 and 2 gives almost the same J_{TAT}, the total J_{TAT} is 2 times as large as each component. It explains why some theoretical papers only considered one between mechanism 1 and 2 and still achieved good fittings to the experimental J_{SILC}. Figure 7(a) and 7(b) present the capture rate from poly-Si (S1) and the total emission rate to poly-Si (S1), oxide and Si substrate (S2). The data in mechanism 1 and 2 almost overlap with

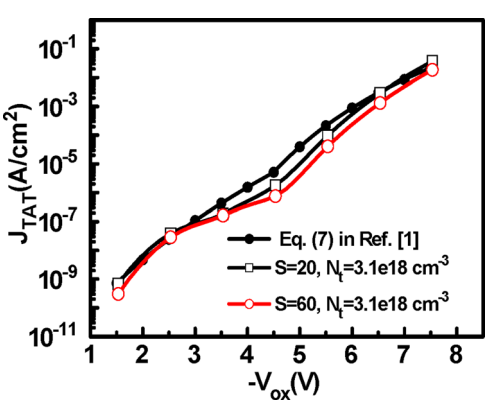

FIG. 6. (Color online) The total J_{TAT} by summing TAT components in both mechanism 1 and 2. The data from the fitting Eq. (7) in Ref. 1 are also shown for comparison.

Downloaded 05 Sep 2013 to 35.8.11.2. This article is copyrighted as indicated in the abstract. Reuse of AIP content is subject to the terms at: http://jap.aip.org/about/rights_and_permissions

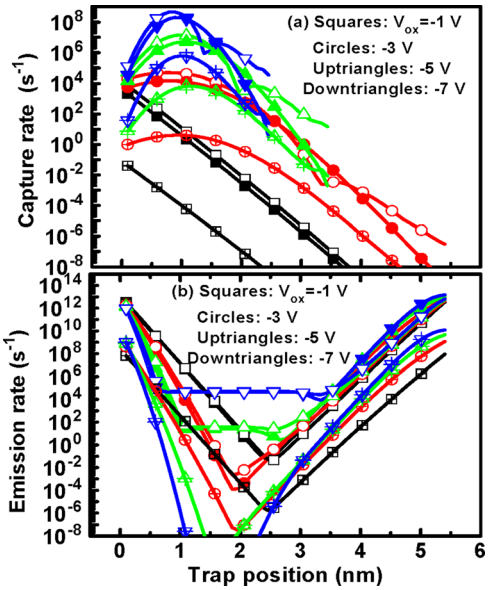

FIG. 7. (Color online) (a) Trap capture rates from poly-Si, and (b) total trap emission rates at four V_{ox} values calculated in three mechanisms. Hollow, solid and cross-symbols stand for mechanism 1, 2, and 3, respectively. The zero of the z coordinate is at the poly-Si/SiO_2 interface.

each other, while the values of capture rate and emission rate in our corrected Schenk's model are much smaller than those in other two mechanisms. From Fig. 7, the shape change of capture or emission rate versus position or oxide voltage is almost the same in three mechanisms, as the tunneling probability is mainly determined by the exponential factor $S'(z_0)$ in Eq. (13) and the emission rate $W_{t,o}$ by $\exp[-(4/3)(\sqrt{2m_{ox}}/\hbar q F_{ox})|E_t|^{3/2}]$ in Eq. (6). Various preexponential factors for transition rates are determined by r_t, F_{ox}, and other quantities. It can be seen from above equations that their dependencies on r_t and F_{ox} are different in three mechanisms. Of them, the preexponential factors for transition rates in Schenk's model (mechanism 3) are much smaller compared to those in other mechanisms.

In order to analyze TAT current, the trap occupation function $f(z)$ and the bulk current generation rate $G_{bulk}(z)$ have been plotted in Fig. 8 under mechanism 1 (M1) at two values of $V_{ox} = -3.53$ and -5.53 V. The first V_{ox} is in the direct tunneling region and the second one is in the FN tunneling region. At $V_{ox} = -3.53$ V, the tunneling current is mostly generated near the center of the oxide, which is $x = 2.95$ nm from the poly-Si/SiO_2 interface. At $V_{ox} = -5.53$ V, the tunneling current generation rate is almost uniform in the range from $x = 0.5$ to 2.5 nm, which follows the shape of $f(z)$. For mechanism 2 (M2), $f(z)$, and $G_{bulk}(z)$ are almost the same as those for M1. Different components of capture and emission rates corresponding to various phonon numbers have been calculated at $V_{ox} = -3.53$ V/$x = 2.95$ nm and $V_{ox} = -5.53$ V/$x = 1.68$ nm in both M1 and M2. The phonon number and the trap energy is related to each other through $E_t = E_{t0} + p\hbar\omega = \hbar^2/(2m_{ox}r_t^2)$, with negative p values for the trap state to absorb phonons and positive p values for the trap to emit phonons. Figures 9(a) and 9(b) show that at the bias position point of $V_{ox} = -3.53$ V/$x = 2.95$ nm, various terms for phonon absorption to the contribution of total capture rate $W_{s1,t}$ and those for phonon emission to the contribution of emission rate $W_{t,s2} + W_{t,o}$, respectively. As this bias-position point is in direct tunneling region, the terms for $W_{t,o}$ are very small. The peak energy difference between phonon emission and absorption is the so-called average relaxation energy E_{relax}. Its value is 2.3 eV for M1:$S = 60/\hbar\omega = 20$ meV, 2.2 eV for M1: $S = 20/\hbar\omega = 60$ meV, 2.0 eV for M2:

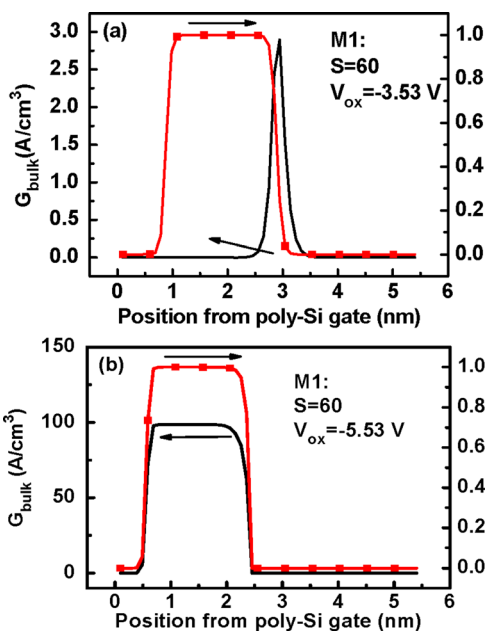

FIG. 8. (Color online) The trap occupation function $f(z)$ and the bulk current generation rate $G_{bulk}(z)$ for the MOS structure with a 5.5 nm SiO_2 in Ref. 1 at (a) $V_{ox} = -3.53$ V, and (b) $V_{ox} = -5.53$ V under mechanism 1 (M1). The product of $S\hbar\omega$ is fixed at 1.2 eV.

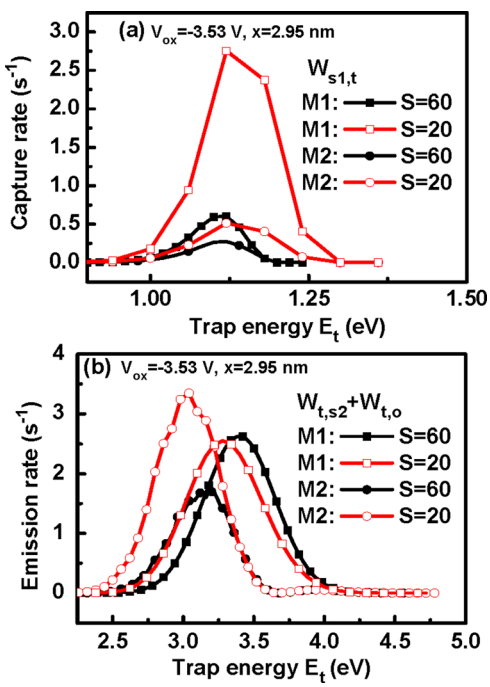

FIG. 9. (Color online) The distribution of various terms of $W_{s1,t}$ vs trap energy due to phonon absorption (a) and emission (b) by the trap in mechanism 1 (M1) and 2 (M2) at the bias-position point of $V_{ox} = -3.53$ V/$x = 2.95$ nm.

Downloaded 05 Sep 2013 to 35.8.11.2. This article is copyrighted as indicated in the abstract. Reuse of AIP content is subject to the terms at: http://jap.aip.org/about/rights_and_permissions

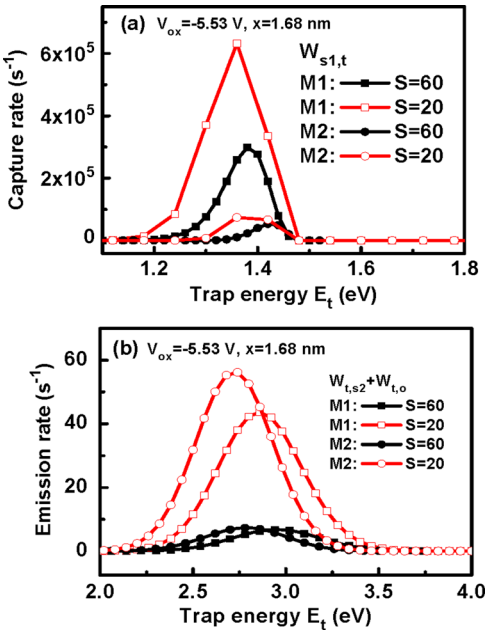

FIG. 10. (Color online) The distribution of various terms of $W_{t,s2} + W_{t,o}$ vs trap energy due to phonon absorption (a) and emission (b) by the trap in mechanism 1 (M1) and 2 (M2) at the bias-position point of $V_{ox} = -5.53$ V/$x = 1.68$ nm.

$S = 60/\hbar\omega = 20$ meV, and 1.9 eV for M2: $S = 20/\hbar\omega = 60$ meV. Therefore, different choices of parameter S and $\hbar\omega$ do not change E_{relax} very much. Figures 10(a) and 10(b) show that at $V_{ox} = -5.53$ V/$x = 1.68$ nm, different terms for phonon absorption to the contribution of total capture rate $W_{s1,t}$ and those for phonon emission to the contribution of emission rate $W_{t,s2} + W_{t,o}$, respectively. Here the terms for $W_{t,o}$ dominate in the emission rate, as this bias-position point is in the FN tunneling region. E_{relax} is 1.6 eV for M1: $S = 60/\hbar\omega = 20$ meV, 1.5 eV for M1: $S = 20/\hbar\omega = 60$ meV, 1.34 eV for M2: $S = 60/\hbar\omega = 20$ meV, and 1.34 eV for M2: $S = 20/\hbar\omega = 60$ meV. These values are smaller than those shown in Fig. 9. It is also observed that compared to the choice of $S = 60/\hbar\omega = 20$ meV, adopting $S = 20/\hbar\omega = 60$ meV increases $W_{t,o}$ by about one order in the FN tunneling region. Figure 11 shows the schematic process of inelastic tunneling due to multiphonon absorption and emission.

In order to further examine the our model, we also fitted the SILC data of Ref. 25 where an inelastic tunneling model had been proposed to explain the stressed induced gate current in an $n+$ poly-Si gate P-MOSFET. The oxide thickness is 5.8 nm. The gate voltage and oxide electric field are related to each other by $V_g = V_{ox} - E_g/q$ (both V_g and V_{ox} are negative for gate injection). Jimenez-Molinos *et al.* had fitted these SILC data using their MP trap assisted tunneling model (mechanism 2 only).[15] Their results are: a neutral trap distribution $N_t(z) = 7.0 \times 10^{19} \times \exp(-z/\lambda)$ cm^{-3} with $\lambda = 2.5$ nm, $E_{t0} = -2.8$ eV, and $S\hbar\omega = 1.2$ eV.[15] It should be pointed out that their calculation did not include the electric field induced trap ionization in a triangle barrier, whose emission rate is described by $W_{t,o}$ in the present paper. We only consider mechanism 1 and 2 in our calculation. Our results are: $N_t(z) = N_0 \times \exp(-z/\lambda)$ with $\lambda = 3.5$ nm, $E_{t0} = -2.3$ eV and $S\hbar\omega = 1.2$ eV. Two choices of $S = 60/\hbar\omega = 20$ meV and $S = 20/\hbar\omega = 60$ meV give $N_0 = 1.0 \times 10^{18}$ cm^{-3} and 1.58×10^{18} cm^{-3}, respectively. The difference in the values of N_0 in two cases is not large. Jimenez-Molinos *et al.* had used a poly-Si gate doping of 5×10^{20} cm^{-3}.[15] This value is too high to reproduce the tunneling current in the fresh device, which we have calculated using the method in Ref. 23 We find that a value of 1×10^{20} cm^{-3} for the $n+$ poly-Si gate doping gives a good fitting. Figure 12 presents our calculated results. The agreement with the experimental SILC data is very good. The inset shows the gate leakage current density in fresh and stressed devices from Ref. 25 and our calculated gate leakage current density in the fresh device. The contributions from mechanism 1 and 2 to TAT current are almost the same as the first example. Figure 13(a) presents that at $V_g = -4.22$ V/$x = 3.0$ nm, different terms for phonon absorption to the contribution of total capture rate $W_{s1,t}$ and those for phonon emission to the contribution of emission rate $W_{t,s2} + W_{t,o}$, respectively. Figure 13(b) gives the corresponding values at the bias-position point of $V_g = -6.62$ V/$x = 1.8$ nm. The data are calculated using mechanism 1 (M1) only. The calculation using mechanism 2 (M2) gives the similar values of rate constants. These two bias-position points are in direct and FN tunneling region, respectively. The trap occupation function $f(z)$ and the bulk

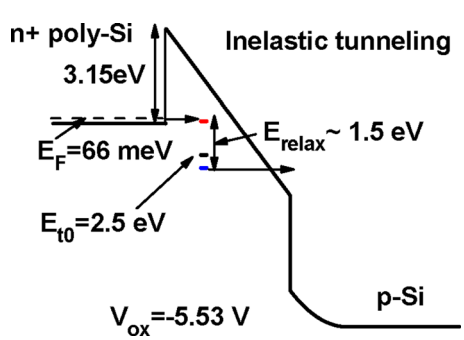

FIG. 11. (Color online) A schematic presentation of the inelastic tunneling process. The average relaxation energy E_{relax} is about 1.5 eV.

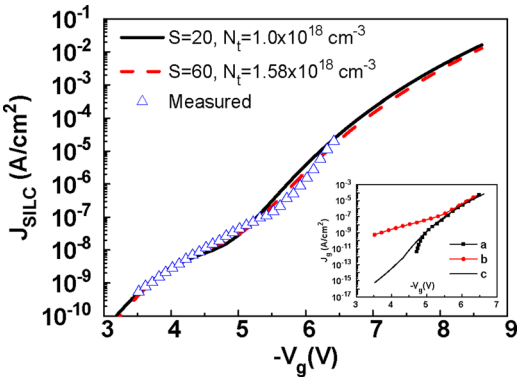

FIG. 12. (Color online) A comparison of SILC density from Ref. 25 and our calculated total multiphonon trap-assisted tunneling current in mechanism 1 and 2. The trap density is fitted to $N_t(z) = N_0 \times \exp(-z/\lambda)$ with $\lambda = 3.5$ nm. Two choices of $S = 60/\hbar\omega = 20$ meV and $S = 20/\hbar\omega = 60$ meV give $N_0 = 1.0 \times 10^{18}$ cm^{-3} and 1.58×10^{18} cm^{-3}, respectively. The insect shows (a) the measured gate leakage current density in the fresh device, (b) the measured total gate leakage current density in the stressed device, and (c) our calculated tunneling current density without TAT in the fresh device using the method in Ref. 22.

Downloaded 05 Sep 2013 to 35.8.11.2. This article is copyrighted as indicated in the abstract. Reuse of AIP content is subject to the terms at: http://jap.aip.org/about/rights_and_permissions

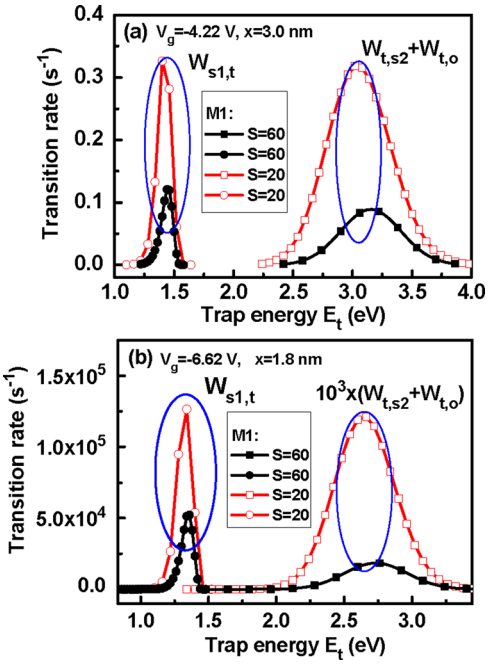

FIG. 13. (Color online) The distribution of various terms of phonon absorption contributing to the total capture rate $W_{s1,t}$ and the distribution of various terms of phonon emission contributing to the emission rate $W_{t,s2}+W_{t,o}$ for the MOS structure with a 5.8 nm SiO_2 in Ref. 25 at two bias-position points of (a) $V_g=-4.22$ V/$x=3.0$ nm and (b) $V_g=-6.62$ V/$x=1.8$ nm in mechanism 1 (M1). The product of $S\hbar\omega$ is fixed at 1.2 eV.

current generation rate $G_{\text{bulk}}(z)$ at these two bias-position points are similar to Fig. 9 and Fig. 10. At $V_g=-4.22$ V/$x=3.0$ nm, E_{relax} is 1.69 eV for $S=60/\hbar\omega=20$ meV, and 1.63 eV for $S=20/\hbar\omega=60$ meV, respectively. At $V_g=-6.62$ V/$x=1.8$ nm, E_{relax} is 1.36 eV for $S=60/\hbar\omega=20$ meV and 1.3 eV for $S=20/\hbar\omega=60$ meV, respectively. So at both bias-position points, E_{relax} is about 1.5 eV.

In above two examples, the value of $E_{\text{relax}}\sim 1.5$ eV is in agreement with the result of a simple inelastic tunneling model in Ref. 25 where E_{relax} is a fitting parameter. Our model of MP TAT gives a direct calculation method for it. A remark can be made about the limitations of the present results as follows. The transition rates associated with all three different mechanisms considered in this work are always proportional to the line shape function, which determinates the temperature dependence of the current. Thus the temperature dependence in all three mechanisms should be very similar in the present scheme. In addition, the value of $S\hbar\omega=1.2$ eV is high, so a very strong temperature dependence of the TAT current should be expected in the present model compared to the one typically observed in SiO_2.[23] There are several choices of $S\hbar\omega$ for traps in SiO_2 in the literature.[12,15,16,20,23] For example, Nasyrov *et al.* have adopted $S\hbar\omega=1.6$ eV with a neutral trap model in their studies of tunneling current in metal-nitride-oxide-silicon structures;[12] Vandelli *et al.* have adopted $S=6/\hbar\omega=60$ meV with a positive trap model in SiO_2 in their study of temperature dependence of gate current in SiO_2/HfO_2 gate stacks.[23] In the near future we will examine the effect of including trap-to-trap tunneling and choosing traps with different trap charge states on the temperature dependence of the TAT current. For Coulomb traps, one must consider the effect of the long-ranged Coulomb potential on the capture and emission rate. The calculation will become complicated. Further extending the present calculation to a positive Coulomb trap is under the way.

V. CONCLUSIONS

In summary, a comparison is made for three multiphonon trap-assisted tunneling mechanisms in the gate leakage current in a MOS structure: the short-ranged trap potential, nonadiabatic interaction and Schenk's electric field induced trap−band transitions. First for the transition induced by the short-ranged trap potential, the difference in the transition matrix elements for the tunneling ionization process between the Price-Sah and Makram-Ebeid-Lannoo model has been explained by Bardeen's method of transfer Hamiltonian method. Then, a properly box-normalized electron wave function in the SiO_2 conduction band in an electric field is proposed. Using this wave function for SiO_2, Lucovsky's wave function for the trap state of a deep neutral trap and the standard effective-mass wave functions for Si cathode and anode, multiphonon assisted capture and emission rates of a deep neutral trap in SiO_2 have been derived. The detailed numerical calculation show that capture and emission rates are almost the same for the mechanism 1 and 2 induced, so the two mechanisms give a similar contribution to the total TAT current. In contrast, capture and emission rates in Schenk's model are smaller. After correcting some drawbacks in the original implementation of Schenk's model, the TAT current induced by this mechanism is even much smaller in the Fowler-Nordheim injection region. The calculated TAT current by considering the first two mechanisms is in good agreement with the experimentally measured stress-induced gate leakage current. The calculated average relaxation energy (~1.5 eV) is in agreement with previous experiments.

ACKNOWLEDGMENTS

This work is supported by National Basic Research Program of China (973 Program) under No. 2010CB934204 and 2011CBA00600; National Natural Science Foundation of China under No. 60825403, 61176080 and 61176073; Hi-Tech Research and Development Program of China (863 Program) under No. 2008AA031403.

[1]E. Rosenbaum and L. F. Register, IEEE Trans. Electron Devices **44**, 317 (1997).
[2]D. Ielmini, A. S. Spinelli, M. A. Rigamonti, and A. L. Lacaita, IEEE Trans. Electron Devices **47**, 1258 (2000).
[3]T. Grasser. H. Reisinger, P.J. Wagner, F. Schanovsky, W. Goes, and B. Kaczer, IEEE International Reliability Physics Symposium (IEEE, Garden Grove, 2010), pp. 16–25.
[4]D. Veksler, G. Bersuker, M. Shur, H. Park, C. Young, K. Y. Lim, W. Taylor, and R. Jammy, IEEE International Reliability Physics Symposium (IEEE, Garden Grove, 2010), pp. 73–79.
[5]I. Lundström and C. Svensson, J. Appl. Phys. **43**, 5045 (1972).
[6]J. Bardeen, Phys. Rev. Lett. **6**, 57 (1961).
[7]D. Vuillaume, J. C. Bourgoin, and M. Lannoo, Phys. Rev. B **34**, 1171 (1986).
[8]C.T. Sah, Phys. Rev. **123**, 1594 (1961).

Downloaded 05 Sep 2013 to 35.8.11.2. This article is copyrighted as indicated in the abstract. Reuse of AIP content is subject to the terms at: http://jap.aip.org/about/rights_and_permissions

[9]V. Karpus and V. I. Perel, Zh. Eksp. Teor. Fiz. **91**, 2319 (1986). [Sov. Phys. JETP **64**, 1376 (1986)].
[10]S. D. Gannichev, W. Prettl, and I. N. Yassievich, Phys. Solid State **39**, 1703 (1997).
[11]S. Makram-Ebeid and M. Lannoo, Phys. Rev. B **25**, 6406 (1982).
[12]K. A. Nasyrov, S. S. Shaimeev. V. A. Gritsenko, and J. H. Han, J. Appl. Phys. **105**, 123709 (2009).
[13]E. Gutsche, Phys. Status Solidi B **109**, 583 (1982).
[14]D. Gguenheim and M. Lannoo, J. Appl. Phys. **68**, 1059 (1990).
[15]F. Jimenez-Molinos, A. Palma, F. Gamiz, J. Banqueri, and J. A. Lopez-Villanueva, J. Appl. Phys. **90**, 3396 (2001).
[16]A. Palma, A. Godoy, J. A. Jimenez-Tejada, J. E. Carceller, and J. A. Lopez-Villanueva, Phys. Rev. B **56**, 9565 (1997).
[17]A. Schenk, R. Enderlein, and D. Suisky, Phys. Status Solidi B **131**, 729 (1985).
[18]G. Lucovsky, Solid State Commun. **3**, 299 (1965).
[19]M. Hermann and A. Schenk, J. Appl. Phys. **77**, 4522 (1995).
[20]A. Gehring and S. Selberherr, "Modeling of wearout, leakage, and breakdown of gate dielectrics," Proceedings of the 11th international symposium on the physical and failure analysis of integrated circuits (IEEE, Taiwan, 2004), pp. 61–64.
[21]F. Schuler, R. Degraeve, P. Hendrickx, and D. Wellekens, IEEE Trans. Electron Devices **2**, 80 (2002).
[22]J. Cai and C. T. Sah, J. Appl. Phys. **89**, 2272 (2001).
[23]L. Vandelli, A. Padovani, L. Larcher, R. G. Southwick, W. B. Knowlton, and G. Bersuker, IEEE Trans. Electron Devices **58**, 2878 (2011).
[24]B. K. Ridley, in *Quantum Processes in Semiconductors*, 4th ed. (Clarendon, Oxford, 1999), p. 257.
[25]S. Takagi, N. Yasuda, and A. Toriumi, IEEE Trans. Electron Devices **46**, 335 (1999).

Downloaded 05 Sep 2013 to 35.8.11.2. This article is copyrighted as indicated in the abstract. Reuse of AIP content is subject to the terms at: http://jap.aip.org/about/rights_and_permissions